Spin-resolved nature of 3s photoemission from ferromagnetic iron

A. K. See and L. E. Klebanoff*
Department of Chemistry and Zettlemoyer Center for Surface Studies, Lehigh University, Bethlehem, Pennsylvania 18015
(Received 24 October 1994)

Spin-resolved and high-energy resolution x-ray photoelectron spectroscopy measurements of the 3s level of metallic Fe are reported. A majority-spin (↑-spin) component, to our knowledge, previously uncharacterized, is identified in the Fe 3s spectra. This component, whose relative intensity increases significantly at higher-photon energies, is assigned to a remnant of the atomic ^1G term of the $4s^2 3d^6$ valence configuration of atomic Fe. The relationship of these results to previous studies is discussed.

I. INTRODUCTION

A great deal of attention has focused on the spectral splitting observed in the 3s x-ray photoelectron spectroscopy (XPS) spectrum of ferromagnetic Fe.[1–8] This interest stems from the challenge to theoretically describe core-level photoemission from atoms with an unfilled valence shell,[9,10] the expected deviations from atomic character for an itinerant metal,[11,12] and the use of XPS spectral structure to extract information about local magnetic properties.[13,14] We report here a spin-resolved x-ray photoelectron spectroscopy (SRXPS) study of the 3s level of ferromagnetic Fe that reveals additional aspects of Fe 3s photoemission and resolves puzzling questions arising from previous studies.

Fadley and Shirley[1] originally assigned the Fe 3s XPS spectral structure to "multiplet splitting" caused by core-valence intra-atomic exchange, as described by the atomic theory of Van Vleck.[15] Subsequent work,[16–21] briefly reviewed in Ref. 21, has examined the 3s multiplet splitting of 3d transition metals and their compounds, particularly the extent of electron transfer from surrounding atoms to the photoexcited atom. Spin-resolved studies[4,5] of the metallic Fe 3s photoemission have generally confirmed the multiplet splitting assignment, while raising interesting additional questions.

Hillebrecht, Jungblut, and Kisker,[4] employing 250-eV synchrotron radiation, reported a strong minority-spin (↓-spin) polarization for the main Fe 3s component at ~91-eV binding energy, and a majority-spin (↑-spin) polarization for the very broad satellite shifted ~4.5 eV to lower binding energy. Interestingly, a well-defined ↑-spin component near the ↓-spin peak at ~91 eV was not observed, contrary to expectations based on atomic multiplet splitting. A very weak shoulder was observed in the $N\uparrow$ spectrum, but was not discussed.[4] The ↑-spin Fe 3s component possessed an exceptionally large width in comparison to the ↓-spin component that could not be readily explained by lifetime considerations.[4] Qui *et al.*[2] have recently reported that the Fe 3s photoemission line shape, observed using a photon energy ($h\nu$) of 250 eV, differs significantly from that observed at higher-photon energies (for example, $h\nu=1253.6$ eV). These workers speculated that the use of a low-photon energy enhances the surface sensitivity of the measurement, with the varying Fe 3s line shapes reflecting differences between the Fe surface and bulk magnetic properties.[2]

We report here a SRXPS investigation of the Fe 3s level that clarifies the spin-dependent nature of Fe 3s photoemission, and also helps to resolve the outstanding questions above. The experimental details, results, discussion, and conclusions are given in Secs. II–V, respectively.

II. EXPERIMENTAL

High-energy-resolution measurements of the metallic Fe 3s level employed Lehigh University's SCIENTA ESCA-300 x-ray photoelectron spectrometer, described elsewhere.[22] The overall spectroscopic energy resolution was 0.32-eV full width at half maximum (FWHM) for the high-resolution studies at $h\nu=1486.67$ eV. For high-resolution study, the Fe sample consisted of a 99.996% pure polycrystalline Fe foil that was scraped in vacuum with a tungsten-carbide blade prior to analysis. The pressure in the analysis chamber during high-resolution measurement was 1.0×10^{-9} Torr.

SRXPS measurements were performed with an instrument described in detail elsewhere.[23] The instrument consists of a V.G. MkII 150° spherical-sector electrostatic energy analyzer coupled to a low-energy diffuse scattering electron-spin detector.[24] During these studies the Sherman function was 0.035 ± 0.003. The photon source was an unmonochromatized Mg Kα (1253.6 eV) x-ray tube operating at 510 W. The overall energy resolution for the SRXPS measurements was 1.6-eV FWHM. The residual pressure in the SRXPS analysis chamber was 2×10^{-10} Torr during data acquisition.

The sample for SRXPS study was a single-crystal Fe(011) film prepared by evaporation of high-purity Fe onto a W(011) substrate.[25] The Fe(011) film was magnetized in the surface plane along the [001] easy axis by passing a current pulse through a magnetizing coil placed alongside the W(011) crystal. The thickness of the Fe metal film was not explicitly measured but was sufficient to completely suppress the W 4f (1220-eV kinetic energy) photoelectrons emanating from the underlying W(011) substrate, indicating that the Fe metal film thickness was in excess of ~80 Å. Photoelectrons were collected along the [001] normal direction with an angular resolution of ±11°. The 30-eV secondary electron-spin polarization was 0.25 ± 0.01, in agreement with previous work.[26] Spin-summed spectra ($N\uparrow+N\downarrow$) were in excellent agreement with conventional XPS spectra taken with the same energy resolution.

Spin-resolved core-level data were collected into four channels N_L^+, N_L^- and N_R^+, N_R^-. Here, N_L^+ represents the number of electrons diffusely scattered to the left (L) from the Au target in the spin detector when the sample magnetization is positive (+). N_R^- is the number of electrons scattered to the right (R) from the Au target when the sample magnetization has been reversed to the negative (−) direction. The electron-beam polarization P can be expressed as[27]

$$P=\frac{1}{S}\left[\frac{\sqrt{N_L^+N_R^-}-\sqrt{N_L^-N_R^+}}{\sqrt{N_L^+N_R^-}+\sqrt{N_L^-N_R^+}}\right], \quad (1)$$

where S is the analyzing power of the spin detector, known as the Sherman function. SRXPS measurements using both (+) and (−) magnetizations removes from the polarization data apparatus asymmetry effects unrelated to the spin of the electron beam. The polarization data can be separated into individual $N\uparrow$ and $N\downarrow$ SRXPS spectra for the majority-spin ($\uparrow$-spin) and minority-spin ($\downarrow$-spin) photoelectons, respectively, using the equations $N\uparrow=2N_{\rm tot}(1+P)$ and $N\downarrow=2N_{\rm tot}(1-P)$, where $N_{\rm tot}=(N_L^+ +N_L^- +N_R^+ +N_R^-)/4$. The statistical error bars ($\pm\delta N\uparrow\downarrow$) shown in the figures are calculated via the expression $\delta N\uparrow\downarrow=N\uparrow\downarrow(1/S\sqrt{4N_{\rm tot}})$. Count rates (summed over the L and R detectors) for the Fe 3s level were approximately 208 s^{-1}, at 510-W x-ray power.

III. RESULTS

Figure 1 displays a high-energy-resolution XPS spectrum of the Fe 3s level. There is no obvious evidence for additional Fe 3s spectral structure beyond that reported previously,[1–3] and except for an improved energy resolution, the data in Fig. 1 agree with previous high-photon-energy Fe 3s XPS data. We found, however, that least-squares fits to this high-resolution data using a single Doniach-Sunjic (DS) line[28] for the main component, a single DS line for the satellite, and a flat linear background did not quantitatively reproduce the experimental spectrum. The satellite-to-main-peak intensity ratio for the semiquantitative two-peak fit was 0.16 with a ΔE_{3s} value of 5.0±0.1 eV, both in good agreement with previous two-peak analyses[2,3] of high-photon-energy data.

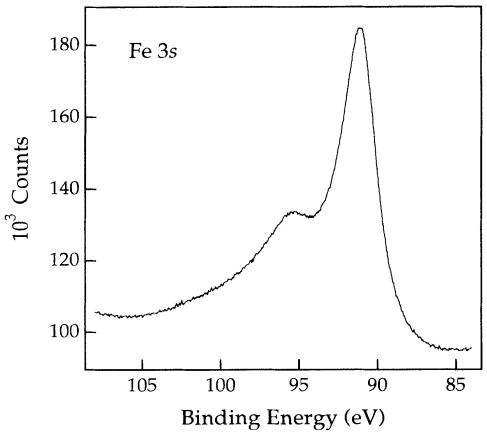

FIG. 1. High-energy-resolution XPS spectrum of the Fe 3s level. The solid line connects the raw experimental data points spaced 0.05 eV apart.

Figure 2(a) presents SRXPS spectra for the Fe 3s level. The solid lines through the raw data represent Savitsky-Golay smooths. The $N\downarrow$ (minority-spin) component (component A), consists of a single peak located at 90.59±0.05-eV binding energy. The $N\downarrow$ component A can be fit very well with a single DS line convoluted with the 1.6-eV FWHM instrumental broadening, giving a Lorentzian broadening Γ of 2.37-eV FWHM, and a singularity index α of 0.16. *In contrast, the $N\uparrow$ Fe 3s SRXPS spectrum clearly consists of a doublet.* A fit to the $N\uparrow$ Fe 3s envelope using two DS line shapes gives a component at 91.42±0.08 eV (component B), and a second $\uparrow$-spin component at 95.05±0.08-eV binding energy (component C). The solid line above the $N\uparrow$ and $N\downarrow$ SRXPS spectra in Fig. 2(a) is the spin-summed spectrum $N\uparrow+N\downarrow$. The Fe 3s intensity ratio $I\downarrow/I\uparrow=I(A)/[I(B)+I(C)]$ is 1.25, close to the $I\downarrow/I\uparrow$ ratio of 1.16±0.1 reported by Hillebrecht, Jungblut, and

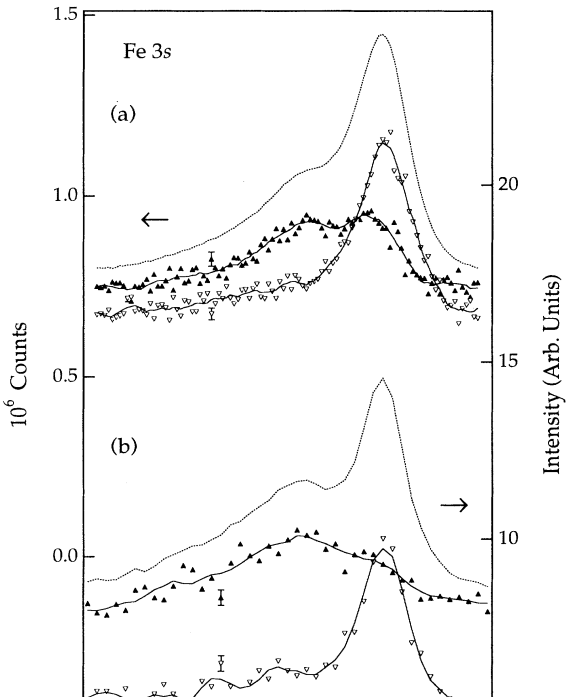

FIG. 2. (a) Separate $N\uparrow$ and $N\downarrow$ SRXPS spectra for the Fe 3s majority-spin (▲) and minority-spin (▽) photoelectrons, respectively. Binding energy is plotted against photoelectron counts (left axis). The line through the raw $N\downarrow$ data is a second-order 11-point Savitzky-Golay (SG) smooth. The line through the $N\uparrow$ data is a second-order, 15-point SG smooth. The dotted line above the SRXPS data is the spin-summed spectrum ($N\uparrow+N\downarrow$). (b) The Fe 3s $N\uparrow$ (▲) and $N\downarrow$ (▽) photoemission spectra of Ref. 4, recorded with 250-eV photon energy. Binding energy is plotted against intensity (right axis) as reported in Ref. 4. The line through the raw $N\downarrow$ data is a fourth-order, 11-point SG smooth. The line through the $N\uparrow$ data is a second-order, 11-point SG smooth. The dotted line is the spin-summed spectrum ($N\uparrow+N\downarrow$) at 250-eV photon energy.

Kisker[4] using 250-eV synchrotron radiation. The raw data from Ref. 4 are shown in Fig. 2(b), with the solid lines through the $N\uparrow$ and $N\downarrow$ data indicating Savitsky-Golay smooths. The spin-summed spectrum $N\uparrow+N\downarrow$ from the Ref. 4 data is also shown in Fig. 2(b).

IV. DISCUSSION

Figure 3 directly compares our high-photon-energy SRXPS Fe 3*s* results with the 250-eV photon energy spin-resolved data of Hillebrecht, Jungblut, and Kisker.[4] For clarity, only the smoothed $N\uparrow$ and $N\downarrow$ curves from Fig. 2 are shown. It is clear from Fig. 3 that the overall Fe 3*s* line shape does vary with photon energy. There is very little change in the Fe 3*s* $N\downarrow$ spin line shape as the photon energy is increased from 250 to 1253.6 eV. However, the $N\uparrow$ Fe 3*s* line shape changes significantly. As the photon energy increases, component *B* evolves from a weak shoulder at low-photon energy to a distinct and prominent $N\uparrow$ component in the Fe 3*s* SRXPS spectrum. The overall width of the Fe 3*s* $N\uparrow$ envelope decreases somewhat with increasing photon energy. The statistical quality of the SRXPS data, the excellent agreement between the two $N\downarrow$ measurements (Fig. 3), and the consistency of our spin-integrated results with previous high-energy spin-integrated studies[2,3] all guarantee that the photon-energy-dependent $N\uparrow$ variations in Fig. 3 are reliable.

The differences observed in Fig. 3 are a true photon-energy dependence, and cannot be attributed to a varying surface sensitivity of high- and low-photon-energy measurements.[2] Using spin-integrated XPS with an angular resolution of $\pm 2.5°$, we have found that the Fe 3*s* line shape recorded for normal emission [effective escape depth ~ 15 Å (Ref. 29)] and 70° off normal [effective escape depth ~ 6 Å (Ref. 29)] showed excellent agreement.

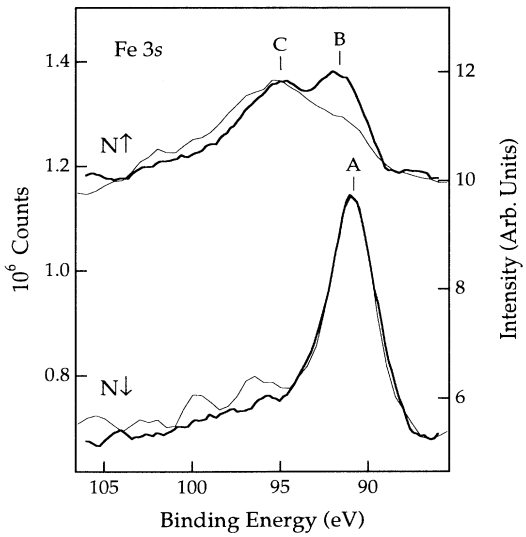

FIG. 3. Thick lines: SG smooth curves of Fig. 2 obtained at $h\nu=1253.6$ eV. The left axis is applicable to the SRXPS data. Thin lines; SG smooth curves of Fig. 2 from the 250-eV synchrotron data of Ref. 4. The right axis is applicable for the data of Ref. 4. The $N\uparrow$ curves have been rigidly shifted vertically (offset) to clarify the presentation. The right axis was scaled so that the two $N\downarrow$ peaks were of equal height. However, the relative intensities within a data set are accurate (i.e., $N\uparrow/N\downarrow$ intensity ratios for the SRXPS data are accurately represented, as are the $N\uparrow/N\downarrow$ intensities for the data from Ref. 4).

The strong increase in the intensity of component *B* at larger photon energies explains puzzling line-shape results from spin-integrated photoemission studies.[2,3] The SRXPS data demonstrate that the satellite-to-main-peak intensity ratio, as gleaned from spin-integrated XPS data, is not a measure of the $N\uparrow/N\downarrow$ intensity ratio, since $\uparrow$-spin component *B* lies on the high-binding-energy side of the $\downarrow$-spin component *A*. The increased prominence of component *B* at high-photon energy causes the satellite-to-main-peak intensity ratio to decrease with increasing photon energy as indicated in previous two-peak fits to the spin-integrated Fe 3*s* line shape.[2,3]

It is observed[2] that the singularity index α for the main Fe 3*s* component increases significantly at higher-photon energies. At $h\nu=1253.6$ eV, the increased prominence of component *B* makes the main 3*s* component (observed in one-peak fits to spin-integrated spectra) much more asymmetric ($\alpha=-0.27$) than the $N\downarrow$ component *A* really is ($\alpha=0.16$). It is probable that experimental variations in the Fe ΔE_{3s} values (from 4.2–4.9 eV) inferred[2,3,7] from two-peak fits to the Fe 3*s* spectrum are attributable in part to the photon-energy dependence of component *B*. The correct value of ΔE_{3s} for metallic Fe is 4.5 ± 0.1 eV.

The comparison in Fig. 3 shows that the photoelectric cross section for peaks *A* and *C* have a similar photon-energy dependence. This similarity, and the opposite spin polarizations for peaks *A* and *C* indicate that peaks *A* and *C* correspond, respectively, to the exchange-split $\langle$HS| and $\langle$LS| final states derived from a $(4sp)^{1.6}3d^{6.4}$ valence configuration.[30] The correct explanation of component *B* must account for its complete $\uparrow$-spin polarization. Surface contamination can be ruled out by XPS checks of the surface cleanliness. The metallic Fe 3*s* $I\uparrow/I\downarrow$ ratio obtained from spin-resolved photoemission at high-photon energy ($I\uparrow/I\downarrow=1.25$, $h\nu=1253.6$ eV) and low-photon energy ($I\uparrow/I\downarrow=1.16$, $h\nu=250$ eV) are similar. This indicates that spin-dependent diffraction is negligible, and does not distort the Fe 3*s* spectral profile. It would in any event be difficult for a spin dependent transport mechanism to increase the prominence of the $\uparrow$-spin peak *B*, but not the $\uparrow$-spin peak *C*.

It has been suggested[18] that for the compound $FeCl_2$, the Fe 3*s* XPS satellite peak is actually a doublet composed of a low-spin ($\langle$LS|) final state derived from a $3d^6$ ($3d^n$) Fe valence configuration and a high-spin ($\langle$HS|) state derived from a charge-transfer-induced $3d^7$ ($3d^{n+1}$) Fe valence configuration. The metallic Fe 3*s* SRXPS data prove conclusively that in Fe metal the components *B* and *C* do not correspond to a $3d^n$ and $3d^{n+1}$ mixture, because one would expect a $\downarrow$-spin polarization for a $\langle$HS| peak derived from a $3d^{n+1}$ valence configuration and a $\uparrow$-spin polarization for a $\langle$LS| peak derived at the $3d^n$ valence configuration. Instead, components *B* and *C* *both* display a pure $\uparrow$-spin polarization.

We believe an atomic model provides a framework in which to understand the spin polarizations of the Fe 3*s* components *A*, *B*, and *C*. We assume that a $4s^23d^6$ atomic configuration approximates the metallic

$(4sp)^{1.6}3d^{6.4}$ valence configuration.[30] Furthermore, since the valence spin polarization for metallic Fe is ~2.1 electrons, we adopt an initial-state atomic spin polarization of 2.0 electrons, corresponding to a triplet ($S=1$) initial state. For the initial state we choose the ^3G term of the $4s^23d^6$ configuration. Photoemission of a 3*s* electron leads to a $^4G(\langle \mathrm{HS}|)$ final state, which we assign to component *A*, and also to a $^2G(\langle \mathrm{LS}|)$ final state, which we assign to component *C*. By conservation of the *z* component of electron spin (m_s),[31] the emission of a ↑-spin 3*s* electron accesses both the ^4G and ^2G final states. The emission of a ↓-spin 3*s* electron accesses only the ^4G final state. So, one has a mixed, but mostly ↓-spin polarization for component *A*, but a pure ↑-spin polarization for peak *C*.

Since component *B* lies only 0.83 eV above component *A*, we do not believe peak *B* represents a 3*d* shakeup transition in which the Fe 3*d* electron count is decreased. Rather we believe peak *B* corresponds, qualitatively, to the excited ^1G atomic term of the atomic $4s^23d^6$ valence configuration. If we couple $(3s^1, {}^2S)$ with $(4s^23d^6, {}^1G)$, we form a single ^2G configuration. The theory of Dembczynksi[32] places the $(4s^23d^6, {}^1G)$ term 0.75 eV higher in energy than the $(4s^23d^6, {}^3G)$ configuration. This energy difference is close to the energy separation between the Fe 3*s* components *A* and component *B*. One would expect this ^2G final state to be accessible only by the photoemission of ↑-spin 3*s* electrons, consistent with the ↑-spin polarization of component *B*. Since peak *B* represents a higher-energy term within the $4s^23d^6$ valence configuration, its intensity may turn on more slowly with photon energy than the components *A* and *C*, which derive from multiplet splitting from the lowest-energy final-state term. The core-valence exchange coupling in metallic Fe can, at best, be only qualitatively described in an atomic model. In this sense, the metallic features *A*, *B*, and *C* can be considered remnants of the atomic terms of the $4s^23d^6$ valence configuration.

V. CONCLUSIONS

SRXPS and high-energy-resolution XPS measurements of the 3*s* level of metallic Fe are reported. An additional ↑-spin component, to our knowledge previously uncharacterized, is identified in the Fe 3*s* spectra. This component, whose relative intensity increases significantly at higher-photon energies, is assigned to a remnant of the atomic ^1G term of the $4s^23d^6$ valence configuration of atomic Fe. The photon energy dependence of this component *B* explains some unusual lineshape variations reported in previous spin-integrated studies.

ACKNOWLEDGMENTS

This paper is based upon work supported by the National Science Foundation under Grant No. CHE-9117138. We acknowledge the time and services of Al Miller in the SCIENTA ESCA Laboratory of Lehigh University. The authors thank Professor Steve Manson for helpful discussions.

*Author to whom all correspondence should be addressed.

[1]C. S. Fadley and D. A. Shirley, Phys. Rev. A **2**, 1109 (1970).
[2]S. L. Qiu, R. G. Jordan, A. M. Begley, X. Wang, Y. Liu, and M. W. Ruckman, Phys. Rev. B **46**, 13 004 (1992).
[3]J. F. Van Acker, Z. M. Stadnik, J. C. Fuggle, H. J. W. M. Hoekstra, K. H. J. Bushow, and G. Stroink, Phys. Rev. B **37**, 6827 (1989).
[4]F. U. Hillebrecht, R. Jungblut, and E. Kisker, Phys. Rev. Lett. **65**, 2450 (1990).
[5]C. Carbone, T. Kachel, R. Rochow, and W. Gudat, Solid State Commun. **77**, 619 (1991).
[6]J. Azoulay and L. Ley, Solid State Commun. **31**, 131 (1979).
[7]D. J. Joyner, O. Johnson, and D. M. Hercules, J. Phys. F **10**, 169 (1980).
[8]C. Binns, C. Norris, G. P. Williams, M. G. Barthes, and H. A. Padmore, Phys. Rev. B **34**, 8221 (1986).
[9]K. Okada, A. Kotani, V. Kinsinger, R. Zimmerman, and S. Hufner, J. Phys. Soc. Jpn. **63**, 2410 (1994).
[10]B. T. Thole and G. van der Laan, Phys. Rev. Lett. **67**, 3306 (1991).
[11]Y. Kakehashi, Phys. Rev. B **32**, 1607 (1985).
[12]Y. Kakehashi and A. Kotani, Phys. Rev. B **29**, 4292 (1984).
[13]F. R. McFeeley, S. P. Kowalczyk, L. Ley, and D. A. Shirley, Solid State Commun. **15**, 1051 (1974).
[14]L. E. Klebanoff and D. A. Shirley, Phys. Rev. B **33**, 5301 (1986).
[15]J. H. Van Vleck, Phys. Rev. **45**, 405 (1934).
[16]V. Kinsinger, I. Sander, P. Steiner, R. Zimmermann, and S. Hufner, Solid State Commun. **73**, 527 (1990).
[17]B. Hermsmeier, C. S. Fadley, M. O. Krause, J. Jimenez-Mier, P. Gerard, and S. T. Manson, Phys. Rev. Lett. **61**, 2592 (1988).
[18]S. J. Oh, G. H. Gweon, and J. G. Park, Phys. Rev. Lett. **68**, 2850 (1992).
[19]B. W. Veal and A. P. Paulikas, Phys. Rev. Lett. **51**, 1995 (1983).
[20]K. Okada and A. Kotani, J. Phys. Soc. Jpn. **61**, 4619 (1992).
[21]D. G. Van Campen and L. E. Klebanoff, Phys. Rev. B **49**, 2040 (1994).
[22]L. E. Klebanoff, D. G. Van Campen, and R. J. Pouliot, Phys. Rev. B **49**, 2047 (1994).
[23]L. E. Klebanoff, D. G. Van Campen, and R. J. Pouliot, Rev. Sci. Instrum. **64**, 2863 (1993).
[24]M. R. Scheinfein, D. T. Pierce, J. Unguris, J. J. McClelland, R. J. Celotta, and M. H. Kelly, Rev. Sci. Instrum. **60**, 1 (1989).
[25]U. Gradmann and G. Waller, Surf. Sci. **116**, 539 (1982).
[26]J. Kirschner and K. Koike, Surf. Sci. **273**, 147 (1992).
[27]J. Kessler, *Polarized Electrons* (Springer-Verlag, Berlin, 1985), p. 234.
[28]S. Doniach and M. Sunjic, J. Phys. C **3**, 285 (1970).
[29]S. Tanuma, C. J. Powell, and D. R. Penn, Surf. Interface Anal. **17**, 911 (1991).
[30]V. L. Moruzzi, J. F. Janak, and A. R. Williams, *Calculated Electronic Properties of Metals* (Pergamon, New York, 1978), p. 8.
[31]S. F. Alvarado and P. S. Bagus, Phys. Lett. **67A**, 397 (1978).
[32]J. Dembczynski, Physica B+C **100C**, 105 (1980).